arXiv:1611.06736v1 [quant-ph] 21 Nov 2016

Quantitative Study of Beam Splitter Generated Entanglement from Input States with Multiple Nonclassicality Inducing Operations

Soumyakanti Bose* and M. Sanjay Kumar†
S. N. Bose National Centre for Basic Sciences
Block-JD, Sector-III, Salt Lake, Kolkata 700106
India.

(Dated: November 22, 2016)

Continuous variable Beam Splitter (BS) generated entanglement from single mode optical states generated by single nonclassicality (**NC**) inducing operation have been found of immense importance in several information processing tasks. There exists a broader class of optical states, generated from successive action of multiple different **NC**-inducing operations, which show many intriguing nonclassical properties; however the BS conversion of the **NC** for such states remains unexplored. In this work we have critically analyzed the BS generated entanglement from such nonclassical optical states at input. Here we present a scenario where BS output entanglement becomes non-monotonic with the input **NC** parameters, amenable experimentally (e.g. number of photon excitation and squeezing strength), in contrast with the previous results with states comprising of single **NC**-inducing operation. We explain this counter intuitive feature in terms of the competition between the **NC**s induced by specific type of **NC**-inducing operations.

Keywords: PACS: 03.67 Bg, 03.67 Mn, 42.50 Ex

I. Introduction

Quantum entanglement plays the central role in various quantum information processing tasks such as quantum communication, quantum computation, *etc* [1]. States having such nonlocal correlation can be easily be obtained from single mode quantum light [2] by using a passive linear device such as beam splitter (BS) [3]. It has been known that a necessary and sufficient criterion for the output states of the BS to be entangled is that atleast one of the input ports be nonclassical [4]. Nonclassical states, are the quantum states of light for which the Glauber-Sudarshan P distribution [5] associated with the density operator ρ,

$$\rho = \int P(\alpha, \alpha^*)|\alpha\rangle\langle\alpha|, \tag{1}$$

fails to be a true probability distribution [6]; where $|\alpha\rangle$ stands for coherent state. Nonclassical states of quantized light can be generated by several **NC**-inducing operations such as photon excitation [7], quadrature squeezing [8], amplitude squeezing [9], *etc*. Thus a quantitative study of BS generated entanglement and input **NC** becomes very important to obtain desired amount of entanglement by tuning experimentally amenable **NC**-inducing parameters.

In recent times, there has been an extensive quantitative and qualitative study [3, 5, 10, 11] of BS generated entanglement for various input nonclassical states with single **NC**-inducing operations such as photon excitation, quadrature squeezing, *etc*. It is worth noting that a quantitative aspect of these studies [3, 10, 11] is that the BS output entanglement grows monotonically with the input **NC**. Nonetheless, there exists a broader class of optical states [12, 13] that are generated under successive action of the two different types of **NC**-inducing operations, *viz.*, namely photon excitation and quadrature squeezing. These states exhibit many intriguing nonclassical effects [14–16]. On the other hand, their two-mode versions are found more entangled than the EPR state $|\psi\rangle_{\rm EPR} = S_{ab}(r)|0\rangle_a|0\rangle_b$ [17] as well as improving the efficiency of teleporting coherent states [18]; $S_{ab}(r) = e^{\frac{r}{2}(a^\dagger b^\dagger - ab)}$ being the two mode correlated squeezing operator. However, the BS generated entanglement from such single mode states remains unexplored. Consequently, it becomes imperative to analyze the BS generated entanglement from such single mode states of light with coexisting multiple different **NC**-inducing operations in the context of quantum information processing tasks with optical resources [19].

In this paper, we study the quantitative aspects of BS generated entanglement from input single mode photon added squeezed vacuum state (PASVS) [13] and squeezed number state (SNS) [12]. We find that the BS output entanglement, from input SNS, depends monotonically on number of photon excitation and quadrature squeezing. On the other hand, for input PASVS, we observe a nonmonotonic dependence on both of them. To understand the specific behavior of entanglement at the BS output, we analyze the input **NC** in terms of well known measures such as nonclassical depth, Hilbert-Schmidt distance from nearest coherent state as well as negativity of Wigner distribution. Our analytical and numerical results show that none of these measures characterize the nonclassical aspects of PASVS and SNS properly to account for corresponding BS output entanglement. Further, to explain this counter-intuitive result, we introduce the concept of competition between the **NC**-inducing operations manifest in terms of Q function contours. We find that, for PASVS, such competition leads to the nonmonotonic entanglement at the BS output, while for SNS the competition is insignificant.

In Section II, we briefly review the known results on BS output entanglement from input states generated by single **NC**-inducing operations, viz., photon addition and quadrature squeezing. In Section II, in contrast to the cases of Section III, we present the dependence of BS entanglement from input states with both the **NC**-inducing operations, in particular, SNS and PASVS. In Section IV, we present a quantitative study of effective **NC** of PASVS and SNS in terms of nonclassical depth, negativity of Wigner distribution as well as Hilbert-Schmidt distance from nearest classical state. In Section V, we propose a picture of these states in terms of contours of Husimi-Kano Q function. We explain the dependence of BS output entanglement on m and r as arising from the competition between the two different **NC**-inducing operations that generate the states.

II. BS Generated Entanglement from Input States Generated under Single NC-Inducing Operations

In this section we focus on the BS generated entanglement from squeezed vacuum state and the photon number state. These states can be viewed as being generated from vacuum state under the action of a single NC-inducing operations such as (i) quadrature squeezing implemented by the squeezing operation $S(r) = e^{\frac{r}{2}(a^{\dagger 2} - a^2)}$ and (ii) photon excitation given by $a^{\dagger m}$. In the squeezed vacuum state, $S(r)|0\rangle$, the variance in the quadrature variable $X = \frac{1}{\sqrt{2}}(a^\dagger + a)$, $V(X) = \langle X^2\rangle - \langle X\rangle^2$, is given by $V(X) = \frac{e^{-r}}{2}$. Hence r can be taken to be a measure of squeezing in the state $S(r)|0\rangle$. It may be noted that $V(X) \leq \frac{1}{2}$ (i.e. $r \geq 0$) implies the state $S(r)|0\rangle$ is nonclassical in the sense that the Glauber-Sudarshan P distribution corresponding to the state is not a true probability distribution. In view of the fact that as r becomes larger and larger, $V(X)$ becomes smaller and smaller compared to $\frac{1}{2}$, it may be argued that higher the value of squeezing strength r, more nonclassical the state $S(r)|0\rangle$ is. In the same way, the photon number state $|m\rangle = \frac{a^{\dagger m}}{\sqrt{m!}}|0\rangle$ is a nonclassical state. Again it is easily argued that the state $|m\rangle$ becomes more nonclassical as m increases as is well known, the Glauber-Sudarshan P distribution becomes more and more singular compared to the delta function [2]. Thus, we see that atleast as far as the action on the vacuum state is concerned, the two NC-inducing operations $S(r)$ and $a^{\dagger m}$ are NC-*increasing* as well. Recently, S. Rahimi-Keshari *et al.* [20] have described the **NC** of any quantum process as whether it induces nonclassical effects on any coherent state $|\beta\rangle$ which is a classical state. Our notion of **NC**-*increasing* operation perfectly corroborates with their definition since the vacuum state can be looked as a special case of $|\beta\rangle$ ($\beta = 0$).

In this background, we now visit the question of how the BS output entanglement $\mathrm{E_{BS}}$ varies with input **NC** when squeezed vacuum state $S(r)|0\rangle$ or photon number state $|m\rangle$ is input at one port of the BS with vacuum $|0\rangle$ at the other. A passive (lossless) 50:50 BS is represented by the transformation matrix

$$\begin{pmatrix} a_{\rm out} \\ b_{\rm out} \end{pmatrix} = \begin{pmatrix} 1/\sqrt{2} & 1/\sqrt{2} \\ -1/\sqrt{2} & 1/\sqrt{2} \end{pmatrix} \begin{pmatrix} a_{\rm in} \\ b_{\rm in} \end{pmatrix} \tag{2}$$

between the input and output modes. For a single mode number state as input BS output state [3] becomes,

$$|n\rangle_{\rm BS}^{\rm out} = |n,0\rangle \xrightarrow{\rm BS} \frac{1}{2^{n/2}} \sum_{k=0}^{n} \binom{n}{k}^{1/2} |n-k,k\rangle. \tag{3}$$

For any bi-partite pure entangled state $|\psi_{\rm AB}\rangle$, entanglement is measured by the local Von-Neumann entropy [1]

$$\mathrm{E}(|\psi_{\rm AB}\rangle) = -\mathrm{Tr}[\rho^{\rm r} ln[\rho^{\rm r}]], \tag{4}$$

where $\rho^{\rm r} = \mathrm{Tr}_A[|\psi_{\rm AB}\rangle\langle\psi_{\rm AB}|]$. BS generated entanglement from input state $|\psi\rangle$ is, thus, obtained by replacing $|\psi_{\rm AB}\rangle$ by $|\psi\rangle_{\rm BS}^{\rm out}$.

Using relation (4), it is easy to show that

$$\mathrm{E}(|n\rangle_{\rm BS}^{\rm out}) = -\sum_{k=0}^{n} \frac{1}{2^n} \binom{n}{k} \log\left[\frac{1}{2^n}\binom{n}{k}\right] \tag{5}$$

while the $\mathrm{E_{BS}}$ for squeezed vacuum state is calculated numerically.

We have evaluated the BS generated entanglement for input number state [Fig. 1(a)] and squeezed vacuum state [Fig. 1(b)]. Clearly, the $\mathrm{E_{BS}}$ increases monotonically as r or m respectively is increased. These results reinforce the argument made above that **NC** of $S(r)|0\rangle$ or $|m\rangle$ increases with r or m respectively because **NC** of the input is a resource from which one has extracted entanglement in the BS setting, as is considered by J. K. Asboth *et al.* [11].

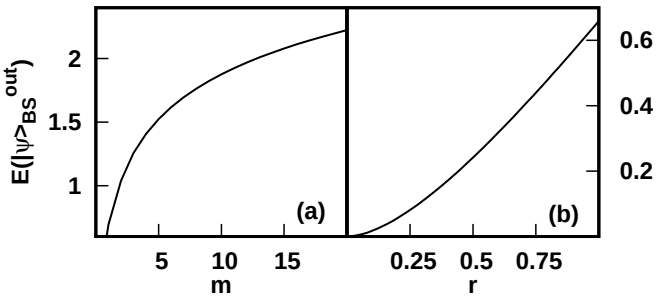

FIG. 1: Entanglement of BS output state with (a) photon number state and (b) squeezed vacuum state as input

III. BS Generated Entanglement from Input States Generated under Two NC-Inducing Operations

Let's now consider successive action of two different NC-inducing operations, *viz.*, quadrature squeezing and

photon addition on an initial vacuum state. This leads to SNS [12] and PASVS [13] given by,

$$|\psi_{\rm SNS}\rangle = S(r)|m\rangle = \frac{S(r)a^{\dagger m}}{\sqrt{m!}}|0\rangle = \sum_{k=0}^{\infty} C_n^m |n\rangle,$$
$$|\psi_{\rm PASVS}\rangle = \frac{1}{\sqrt{N_m}} a^{\dagger m} S(r)|0\rangle, \quad (6)$$

where $N_m = m!\mu^m P_m(\mu)$, $P_n(x) = n^{th}$ order Legendre Polynomial and C_n^m are given in [21].

We now turn to the question of quantitative aspects of BS output entanglement when either SNS or PASVS is input at one of the ports of the BS. Using relation (3) we get the BS output states for input SNS and PASVS as,

$$|\psi_{\rm SNS}\rangle_{\rm BS}^{\rm out} = \sum_{n=0}^{m} C_n^m \frac{1}{2^{n/2}} \sum_{p=0}^{n} \binom{n}{p}^{1/2} |n-p,p\rangle,$$
$$|\psi_{\rm PASVS}\rangle_{\rm BS}^{\rm out} = \frac{1}{\sqrt{N_m}} \sum_{k=0}^{\infty} \frac{\sqrt{(2k+m)!}}{k!} \Big(\frac{\tau}{2}\Big)^k \frac{1}{2^{k+\frac{m}{2}}} \sum_{p=0}^{2k+m} \binom{2k+m}{p}^{1/2} |2k+m-p,p\rangle. \quad (7)$$

In Fig. 2(a), we have plotted the entanglement entropy of the BS output state $|\psi_{\rm SNS}\rangle_{\rm BS}^{\rm out}$ when SNS is input, as a function of r for various values m. One can see from the figure that entanglement increases monotonically with both r as well as m. this monotonic dependence is quite similar to what one had when either a squeezed vacuum state or a photon number state as input as discussed in section II. In contrast, the BS output entanglement with PASVS as input [Fig. 2(b)] shows (except in the case of $m = 1$) a *non-monotonic* dependence on both r and m. For a fixed value of m (> 1), the BS output entanglement first decreases and then increases. For sufficiently large r in fact $\mathrm{E}(|\psi_{\rm PASVS}\rangle_{\rm BS}^{\rm out})$ is almost independent of the photon addition number m.

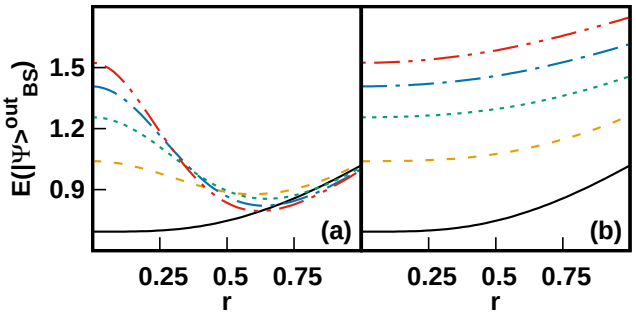

FIG. 2: (Color Online) $E(|\Psi\rangle_{\rm BS}^{\rm out})$ for **a**: PASVS, **b**: SNS] with r for $m = 1$ (black, solid line), 2 (brown, dashed line), 3 (green, dotted line), 4 (blue, dashed-dotted line) and 5 (red, dashed-double dotted line).

From comparison of the results in the cases of SNS and PASVS, it is evident that the dependence of BS output on r and m depends critically on the order of in which the squeezing $[S(r)]$ and the photon addition $[a^{\dagger m}]$ operations act on the initial vacuum state. This non-monotonic dependence in the case of PASVS is indeed counter-intuitive given that (as we have noted in Section II), BS input states generated under a single NC-inducing operation lead to monotonically increasing BS output entanglement.

IV. Effective Single Mode NC Generated under two NC-Inducing Operations

In a first attempt to resolve this non-monotonic dependence mentioned above, we argue that for states generated under multiple NC-inducing operations, SNS and PASVS in particular, r and m individually may not measure nonclassicality of these states, but one should perhaps work with an effective measure. Several nonclassicality measures have been proposed in the literature such as nonclassical depth [22], Wigner negativity [24] and one based on the Hilbert-Schmidt distance [25]. In this Section we shall investigate if any of these measures faithfully capture the **NC** of these states, and if they do, working with such effective measures allows us to understand this non-monotonic dependence.

A. Nonclassical Depth

Nonclassical depth of any quantum state of light is defined as the minimal smoothing needed to wash out the negativity (and singularity) of P distribution. From P distribution one can define a general η convoluted distribution, $R(z,\eta) = \frac{1}{\eta}\int \frac{d^2\omega}{\pi} e^{-\frac{|z-\omega|^2}{\eta}} P(\omega)$. The nonclassical depth, $\eta_{\rm min}$, is defined as the minimum value of η needed to make $R(z,\eta)$ positive semi-definite regular function [22].

The function $R(z,\eta)$ for PASVS and SNS (Appendix A) are given as,

$$R(z,\eta)_{\rm PASVS} = \frac{A_1^m e^{\frac{|z|^2}{1-\eta}} W_0(z,z^*,\eta)}{\mu N_m \sqrt{\eta^2-\tau^2(1-\eta)^2}} \sum_{k=0}^{m} \frac{(-1)^m m!}{k!(m-k)!} \Big(\frac{D_1}{A_1}\Big)^k L_{m-k}\Big(\frac{|B_1|^2}{4A_1}\Big),$$
$$R(z,\eta)_{\rm SNS} = \frac{A_2^m e^{\frac{|z|^2}{1-\eta}} W_0(z,z^*,\eta)}{\mu \sqrt{\eta^2-\tau^2(1-\eta)^2}} \sum_{k=0}^{m} \frac{(-1)^{m-k} m!}{k!(m-k)!} \Big(\frac{D_2}{A_2}\Big)^k L_{m-k}\Big(\frac{|B_2|^2}{4A_2}\Big), \quad (8)$$

where

$$W_0(z,z^*,\eta) = exp\Big(-\frac{\frac{\eta}{1-\eta}|z|^2 - \frac{\tau}{2}[z^2+z^{*2}]}{\eta^2-\tau^2(1-\eta)^2}\Big),$$
$$A_1 = \frac{\tau(1-\eta)^2}{2[\eta^2-\tau^2(1-\eta)^2]}\ ,\ A_2 = \frac{A_1}{\mu^2} - \frac{\tau}{2},$$

$$B_1 = \frac{\eta z - \tau(1-\eta)z^*}{\eta^2 - \tau^2(1-\eta)^2}\ ,\ B_2 = \frac{B_1}{\mu},$$
$$D_1 = \frac{\eta(1-\eta)}{\eta^2 - \tau^2(1-\eta)^2}\ ,\ D_2 = \frac{D_1}{\mu^2}, \tag{9}$$

and $\mu = \cosh r,\ \tau = \tanh r,$ and $L_n(x)$ is the n^{th} order Laguerre polynomial.

Because of the presence of Laguerre polynomial (*eqn.* 8), positiveness of the function $R(z,\eta)$ is not guaranteed for all choices of η. In such cases, as prescribed in [22], the nonclassical depth has to be taken to be unity. Thus we have a situation where nonclassical depth for both $|\psi_{\text{SNS}}\rangle$ and $|\psi_{\text{PASVS}}\rangle$ is the same as the photon number state, and hence it is independent of the squeezing strength r. Clearly, therefore, nonclassical depth fails to be a faithful measure of NC as far as these states are concerned. Further, our conclusion, specifically in the context of these states, is in conformity with the general conclusion that nonclassical depth is always unity for all non-Gaussian pure states [23].

B. Negativity of Wigner Function

It is well known that Wigner function $W_\rho(z,z^*)$ of any state of light ρ, being negative in phase-space, indicates that the state ρ is nonclassical. This criterion of course fails for Gaussian states. Phase space integral of the negative part of the Wigner function, the Wigner negativity

$$\delta = \frac{\int \frac{d^2z}{\pi}|W_\rho(z,z^*)| - 1}{2}, \tag{10}$$

may be considered as a measure of NC [24]. A larger δ implies that the state is more nonclassical.

The Wigner functions of PASVS and SNS (Appendix B) are given by,

$$W_{\text{SNS}}(\alpha,\alpha^*) = (-1)^m e^{-2|\beta|^2} L_m(4|\beta|^2),$$
$$W_{\text{PASVS}}(\alpha,\alpha^*) = \frac{2(-1)^m m! e^{-2|\beta|^2}\mu^m\nu^m}{2^m N_m}\sum_{k=0}^{m}\frac{m!(\frac{\tau}{2})^{-k}}{k!(m-k)!} L_{m-k}\Big(\frac{2|\beta|^2}{\tau}\Big), \tag{11}$$

where $\mu = \cosh r, \nu = \sinh r, \beta = \mu\alpha - \nu\alpha^*$.

In Fig. 3, the Wigner negativity of PASVS is plotted as a function of the squeezing strength r for various values of the photon addition number m. For all values of m, the Wigner negativity falls off with increasing r. This can be understood as being due to photon addition operation for large r. In the case of SNS, however, Wigner negativity is independent of r and hence it is the same as that of the number state $|m\rangle$. The independence of Wigner negativity on r, in case of SNS, can be easily understood from the following fact. If $W_\rho(x,p)$ is the Wigner function of a given state ρ, then the Wigner function of the state $\rho' = S(\zeta)\rho S^\dagger(\zeta)$ is $W_\rho(x',p')$ where x',p' and x,p are related to each other by a linear canonical transformation.

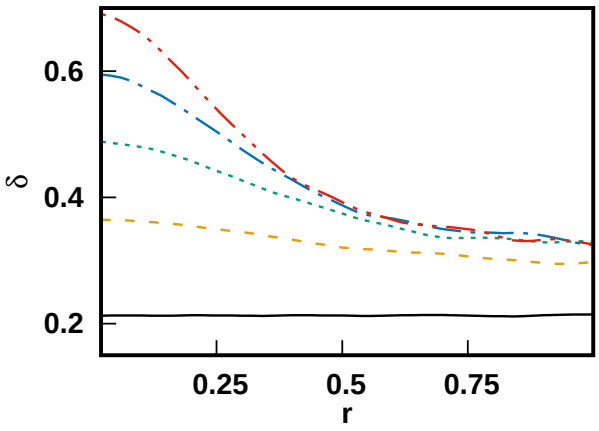

FIG. 3: (Color Online) Dependence of δ with r for m=1 (black, solid line), 2 (brown, dashed line), 3 (green, dotted line), 4 (blue, dashed-dotted line) and 5 (red, dashed-double dotted line) for PASVS.

Since the Jacobian of any linear canonical transformation is unity, the Wigner negativity of $\rho \to \rho'$ are the same.

As in the case of nonclassical depth, again we have a situation where Wigner function negativity fails to be a faithful measure of **NC** as far as SNS is concerned. As our aim is to do a comparative study of PASVS and SNS in the context of entanglement of BS output state with these states as input, it is desirable that we have a measure of **NC** that works equally well for both the **NC**-inducing operations, i.e. photon excitation and quadrature squeezing.

C. Hilbert-Schmidt Distance From Nearest Coherent State

A measure of NC based on the Hilbert-Schmidt distance between density operators has been proposed in the literature [25]. This measure is defined as the Hilbert-Schmidt distance of a given density operator ρ from the nearest classical state. Since coherent states $|\beta\rangle$ are the only pure classical states $|\beta\rangle$ [26], d_{NC} for a pure state $|\psi\rangle$ is defined as,

$$d_{\text{NC}} = \inf\sqrt{2}[1 - \langle\beta|\psi\rangle]^{1/2}. \tag{12}$$

where infimum is taken over set of all coherent states $|\beta\rangle$; β being a complex number.

We have calculated d_{NC} for the two states PASVS and SNS. While d_{NC} for PASVS has a closed form analytic expression given by

$$d_{\text{NC}}\Big)_{\text{PASVS}} = \sqrt{2}\Big[1 - \frac{m^m e^{-m}}{(1-\tau)^m N_m}\Big]^{\frac{1}{2}}, \tag{13}$$

the measure d_{NC} for SNS, can at best be reduced to the simple form

$$d_{\text{NC}}\Big)_{\text{SNS}} = \inf_\beta \sqrt{2}\Big[1 - \frac{\tau^m e^{-|\beta|^2 + \frac{\tau}{2}(\beta^2+\beta^{*2})}}{\mu 2^m} L_m\Big(\frac{|\beta|^2}{2\mu\nu}\Big)\Big]^{\frac{1}{2}}, \tag{14}$$

from where the computation proceeds via a numerical optimization.

In Fig. 4(a) and Fig. 4(b) we have plotted $d_{\rm NC}$ for PASVS and SNS. As is evident from the figures $d_{\rm NC}$ (unlike nonclassical depth and Wigner negativity) shows non-trivial dependence on m and r in the case of both the states. In fact, $d_{\rm NC}$ for both these states exhibits non-monotonic dependence on r and m. However, a comparison of Figs. 3(a) with Figs. 2(a) in the case of PASVS suggests that even for $m = 1$ while **NC** as measured by $d_{\rm NC}$ *decreases* for small r BS output entanglement *increases*. In the case of SNS as well, while the dependence of $d_{\rm NC}$ on r for various m is non-monotonic, the dependence of BS output entanglement is strictly monotonic. In both cases we have unphysical results. This leads us to the conclusion that $d_{\rm NC}$ too is not an acceptable measure of **NC** of states generated under multiple **NC**-inducing operations, in particular SNS and PASVS.

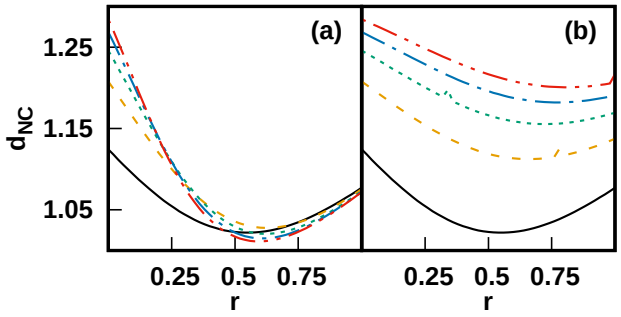

FIG. 4: (Color Online) Dependence of $d_{\rm NC}$ for **a**: PASVS, **b**: SNS with r for m=1 (black, solid line), 2 (brown, dashed line), 3 (green, dotted line), 4 (blue, dashed-dotted line) and 5 (red, dashed-double dotted line)

.

It appears from the above discussion that none of the three measures considered above is an acceptable measure of **NC** of such states. Whether it is possible to construct another measure for such states that shows a dependence on r and m that is consistent with the dependence of BS output entanglement on these parameters remains an open question.

V. Monotonicity vs Non-monotonicity question - Role of competing Nonclassicalities

In this Section we shall attempt to understand the monotonic dependence (in SNS) of BS output entanglement as opposed to the non-monotonic dependence (in the case of PASVS) in terms of a 'competition' between two different kinds of **NC**-inducing operations underlying these states.

To begin with, it is helpful to visualize the effect of the two **NC**-inducing operations acting individually on an initial vacuum state in terms of the deformation induced in the circular Q function contour of the vacuum state. As is well-known light (initially in a coherent state) propagating through a medium with a Kerr nonlinearity undergoes radial squeezing [27], and hence the photon number state can be thought of as an extreme case of a radially squeezed state. Thus, figuratively speaking, the photon excitation (addition) operation $[(a^\dagger)^m]$ can be thought of as deforming the circular Q function contour of the vacuum state into an extreme crescent shape. On the other hand, the squeezing operation $[S(r)]$ can be thought of as deforming the initial circular Q function contour of the vacuum state into an ellipse [28].

The above picture can now be applied to states with two **NC**-inducing operations applied in succession. In the case of PASVS, we plot the contour of Q function in Fig. 5. For small r (= 0.10), with increase in m (a1-a2-a3-a4-a5) Q distribution contours of initial squeezed vacuum state become more of crescent shape showing the dominance of photonic character.

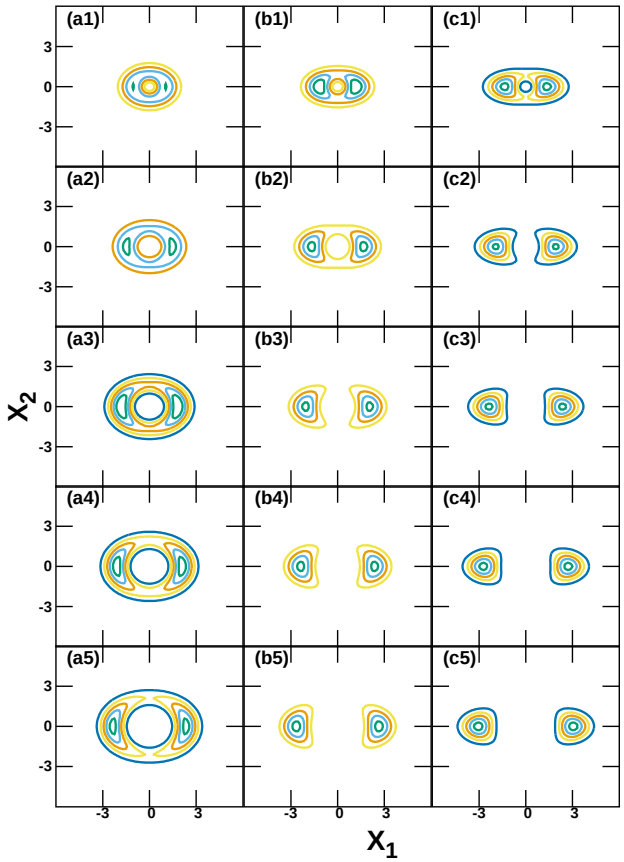

FIG. 5: (Color Online) Contour Plots of Q function for PASVS for a1−c1: $m = 1$ (a1: $r = 0.10$, b1: $r = 0.30$, c1: $r = 0.50$), a2−c2: $m = 2$ (a2: $r = 0.10$, b2: $r = 0.30$, c2: $r = 0.50$), a3−c3: $m = 3$ (a3: $r = 0.10$, b3: $r = 0.30$, c3: $r = 0.50$), a4−c4: $m = 4$ (a4: $r = 0.10$, b4: $r = 0.30$, c4: $r = 0.50$), a5−c5: $m = 5$ (a5: $r = 0.10$, b5: $r = 0.30$, c5: $r = 0.50$). Quadrature components are given as $X_1 = \frac{\beta+\beta^*}{\sqrt{2}}$, $X_2 = \frac{\beta-\beta^*}{i\sqrt{2}}$.

Besides, for moderate squeezing strength ($r \sim 0.30$), while photon excitation introduces radial squeezing, $S(r)$ squeezes the X_1 quadrature leading to an apparent com-

petition between the two specific **NC**-inducing operations, i.e. photon excitation and quadrature squeezing. As a consequence of this competition, contour curves of Q function get bifurcated depending upon the value of m that decides the strength of radial squeezing Fig. 5 (b1-b2-b3-b4-b5). Increasing r further (≥ 0.50), for higher m (≥ 2), we observe that the distance between the bifurcated peaks increases with m (c1-c2-c3-c4-c5). We also note that, for all m values, the crescent shape gets smoothed out with increase in r revealing the dominant squeezing character in the state. Evidently, with increase in r, PASVS undergoes a characteristic crossover, from photonic to quadrature squeezed one. Such characteristic crossover, in the context of competition between photon addition and quadrature squeezing, further explains the specific dependence of E_{BS} on m at fixed r. Since, higher photon excitation makes the state more photonic, in the intermediate region ($0.30 \leq r \leq 0.80$), one can intuitively argue that high m states show less effective **NC** and hence E_{BS} compared to the case of lower m for fixed r, while beyond a critical r (~ 1.0) E_{BS} becomes dependent solely on the squeezing strength r.

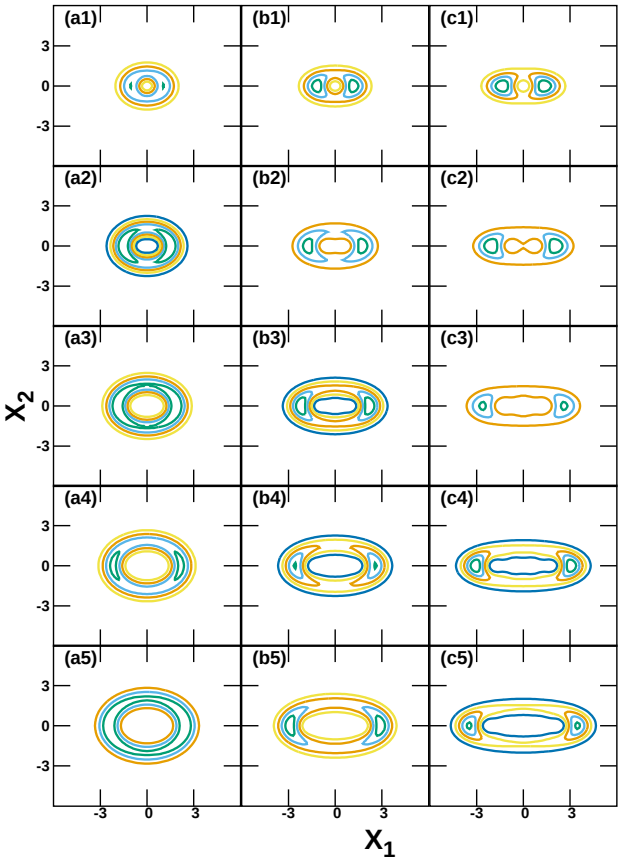

FIG. 6: (Color Online) Contour Plots of Q function for SNS for a1−c1: $m = 1$ (a1: $r = 0.10$, b1: $r = 0.30$, c1: $r = 0.50$), a2−c2: $m = 2$ (a2: $r = 0.10$, b2: $r = 0.30$, c2: $r = 0.50$), a3−c3: $m = 3$ (a3: $r = 0.10$, b3: $r = 0.30$, c3: $r = 0.50$), a4−c4: $m = 4$ (a4: $r = 0.10$, b4: $r = 0.30$, c4: $r = 0.50$), a5−c5: $m = 5$ (a5: $r = 0.10$, b5: $r = 0.30$, c5: $r = 0.50$).

We find, for PASVS, $0.30 \leq r \leq 0.60$ is the parameter region where the effect of competition between elliptic and radial squeezing dominates. It is this effect of competition therefore which can be argued as contributing to the non-monotonic dependence in the BS output entanglement as can be seen from Fig. 2(a).

On the other hand, in the case of SNS, such competitive situation is very much absent. Quadrature squeezing induces elliptic squeezing on the already extreme crescent shape of the Q function contour of the initial photon number state. As is shown in Fig. 6, Here, we observe the radial squeezing for lower r as well as the distant peaks with non-zero interference term for higher r (≥ 0.20) for all m. Consequently, the competitive effect of quadrature squeezing on initial photon excitation is insignificant. This explains why there is no non-monotonicity in this case as is evident from Fig. 2(b).

However, the apparent similarity between PASVS and SNS for $m = 1$ can be explained in terms of the fidelity (F) between these states. For $m = 1$,

$$|\psi_{\rm PASVS}\rangle = \frac{a^\dagger S(r)|0\rangle}{\mu} = \frac{S(r)(\mu a^\dagger + \nu a)|0\rangle}{\mu} = S(r)|1\rangle \tag{15}$$

On the other hand, for $m = 2$,

$$\begin{aligned}|\psi_{\rm PASVS}\rangle &= \frac{a^{\dagger 2} S(r)|0\rangle}{\mu\sqrt{2(3\mu^2-1)}} = \frac{S(r)(\mu a^\dagger + \nu a)^2|0\rangle}{\mu\sqrt{2(3\mu^2-1)}} \\ &= \frac{S(r)(\mu^2 a^{\dagger 2} + \mu\nu(2a^\dagger a + 1))|0\rangle}{\mu\sqrt{2(3\mu^2-1)}} \\ &= \frac{1}{\mu\sqrt{2(3\mu^2-1)}}(\mu\sqrt{2}S(r)|2\rangle + \nu S(r)|0\rangle)\end{aligned} \tag{16}$$

which is superposition of two different squeezed number states, namely, $S(r)|2\rangle$ and $S(r)|0\rangle$. As m increases, PASVS contains superposition of more SNSs. Thus with increase in m, PASVS differs more from SNS as observed in Fig. 2(a) as well as Fig. 4(a). In general, It can be easily shown that,

$$F = |\langle\psi_{\rm PASVS}|\psi_{\rm SNS}\rangle|^2 = \frac{\mu^m}{P_m(\mu)};\ \mu = \cosh r \tag{17}$$

Evidently, $\lim r \to 0 \Rightarrow F \to 1.0$ as well as $\lim m \to 0 \Rightarrow F \to 1.0$.

VI. Conclusion

In conclusion, we have quantitatively studied the BS output entanglement for states generated from successive application of two different NC-inducing operations that lead to in particular to SNS and PASVS. We have observed that while BS output entanglement shows a monotonic dependence on squeezing strength and number of photon addition in the case of SNS, this dependence is non-monotonic in the case of PASVS. We notice that any

attempt to understand this issue of monotonicity vs non-monotonicity fails since none of the measures such as non-classical depth, Wigner negativity and Hilbert-Schmidt distance prove to be acceptable measures of **NC** of these states. We have offered an intuitive picture in terms of Q function contours of these states and pointed out that competition between the two different **NC** inducing operations involved is the key to understand the monotonicity vs non-monotonicity issue.

Appendix A: $R(z,\eta)$ for PASVS and SNS

In general, the η convoluted function $R(z,\eta)$ is defined as,

$$R(z,\eta) = \frac{1}{\eta}\int \frac{d^2\gamma}{\pi} P(\gamma) e^{-\frac{|z-\gamma|^2}{\eta}}. \tag{18}$$

Introducing the expression of $P(\gamma)$ in terms of density operator ρ,

$$P(\gamma) = e^{|\gamma|^2}\frac{1}{\eta}\int \frac{d^2\beta}{\pi}\langle -\beta|\rho|\beta\rangle e^{|\beta|^2} e^{\gamma\beta^* - \gamma^*\beta}, \tag{19}$$

$R(z,\eta)$ can be directly written in terms of ρ as,

$$R(z,\eta) = \frac{e^{\frac{|z|^2}{1-\eta}}}{1-\eta}\int \frac{d^2\beta}{\pi}\langle -\beta|\rho|\beta\rangle e^{-\frac{(2\eta-1)|\beta|^2+(z^*\beta - z\beta^*)}{1-\eta}}. \tag{20}$$

For PASVS, we have

$$\langle\beta|\psi_{\rm PASVS}\rangle = \frac{\beta^{*m}}{\sqrt{\mu N_m}} e^{-\frac{|\beta|^2}{2}+\frac{\tau}{2}\beta^2}. \tag{21}$$

Thus, the $R(z,\eta)$ for PASVS becomes,

$$\begin{aligned} R(z,\eta)_{\rm PASVS} &= \frac{1}{1-\eta} e^{\frac{|z|^2}{1-\eta}} \int \frac{d^2\beta}{\pi}\langle -\beta|\psi_{\rm PASVS}\rangle\langle\psi_{\rm PASVS}|\beta\rangle exp\Big(-\frac{(2\eta-1)|\beta|^2+(z^*\beta - z\beta^*)}{1-\eta}\Big) \\ &= \frac{1}{\mu N_m(1-\eta)} e^{\frac{|z|^2}{1-\eta}} \int \frac{d^2\beta}{\pi}(-|\beta|^{2m}) exp\Big(-\frac{\eta}{1-\eta}|\beta|^2 + \frac{\tau}{2}(\beta^2+\beta^{*2}) - \frac{z^*}{1-\eta}\beta + \frac{z}{1-\eta}\beta^*\Big) \end{aligned}$$

One can derive above non-Gaussian integral using parametric differentiation as,

$$\begin{aligned} R(z,\eta)_{\rm PASVS} &= \frac{(-1)^m}{\mu N_m(1-\eta)} e^{\frac{|z|^2}{1-\eta}} \partial_a^m \partial_b^m \Big[exp\Big(-\frac{\eta}{1-\eta}|\beta|^2 + \frac{\tau}{2}(\beta^2+\beta^{*2}) - \frac{z^*}{1-\eta}\beta + \frac{z}{1-\eta}\beta^*\Big) \\ &\qquad exp\Big(a\beta + b\beta^*\Big)\Big]_{a=0,b=0} \\ &= \frac{(-1)^m}{\mu N_m(1-\eta)} e^{\frac{|z|^2}{1-\eta}} \partial_a^m \partial_b^m \Big[\int \frac{d^2\beta}{\pi} exp\Big(-\frac{\eta}{1-\eta}|\beta|^2 + \frac{\tau}{2}(\beta^2+\beta^{*2})\Big) \\ &\qquad exp\Big((a - \frac{z^*}{1-\eta})\beta + (b + \frac{z}{1-\eta})\beta^*\Big)\Big]_{a=0,b=0} \end{aligned}$$

For any Gaussian integral, we know that

$$\int \frac{d^2z}{\pi} e^{\zeta|z|^2 + \xi z + \eta z^* + f z^2 + g z^{*2}} = \frac{e^{\frac{-\zeta\xi\eta + f\eta^2 + g\xi^2}{\zeta^2 - 4fg}}}{\sqrt{\zeta^2 - 4fg}}. \tag{22}$$

provided $\zeta^2 - 4fg > 0$. Using this formula (18), we get,

$$\begin{aligned} R(z,\eta)_{\rm PASVS} &= \frac{A_1^m e^{\frac{|z|^2}{1-\eta}}}{\mu N_m\sqrt{\eta^2 - \tau^2(1-\eta)^2}} W_0(z,z^*,\eta)\partial_a^m\partial_b^m\Big[e^{A_1a^2 + B_1a - B_1^* + D_1ab + A_1b^2}\Big]_{a=0,b=0} \\ &= \frac{A_1^m e^{\frac{|z|^2}{1-\eta}}}{\mu N_m\sqrt{\eta^2 - \tau^2(1-\eta)^2}} W_0(z,z^*,\eta)\sum_{k=0}^{m}(-1)^m\frac{m!}{k!(m-k)!}\Big(\frac{D_1}{A_1}\Big)^k L_{m-k}\Big(\frac{|B_1|^2}{4A_1}\Big). \end{aligned} \tag{23}$$

where,

$$W_0(z,z^*,\eta) = exp\Big(-\frac{\frac{\eta}{1-\eta}|z|^2 - \frac{\tau}{2}(z^2+z^{*2})}{\eta^2-\tau^2(1-\eta)^2}\Big),\ A_1 = \frac{\tau(1-\eta)^2}{2[\eta^2-\tau^2(1-\eta)^2]}$$
$$B_1 = \frac{\eta z - \tau(1-\eta)z^*}{\eta^2-\tau^2(1-\eta)^2},\ D_1 = \frac{\eta(1-\eta)}{\eta^2-\tau^2(1-\eta)^2} \tag{24}$$

Similarly, using the technique of parametric differentiation and standard Gaussian integral, one can easily derive $R(z,\eta)$ for an SNS. For SNS,

$$\langle\beta|\psi_{\rm SNS}\rangle = \frac{e^{-\frac{|\beta|^2}{2}+\frac{\tau}{2}\beta^{*2}}}{\sqrt{\mu m!}}\partial_a^m\Big[e^{-\frac{\tau}{2}a^2+\frac{\beta^*}{\mu}a}\Big]_{a=0}. \tag{25}$$

Thus we get,

$$\begin{aligned}
R(z,\eta)_{\rm SNS} &= \frac{1}{1-\eta}e^{\frac{|z|^2}{1-\eta}}\int\frac{d^2\beta}{\pi}\langle-\beta|\psi_{\rm SNS}\rangle\langle\psi_{\rm SNS}|\beta\rangle exp\Big(-\frac{(2\eta-1)|\beta|^2+(z^*\beta-z\beta^*)}{1-\eta}\Big)\\
&= \frac{e^{\frac{|z|^2}{1-\eta}}}{\mu m!(1-\eta)}\partial_a^m\partial_b^m\Big[exp\Big(-\frac{\tau}{2}(a^2+b^2)\Big)\\
&\qquad\int\frac{d^2\beta}{\pi}exp\Big(-\frac{\eta}{1-\eta}|\beta|^2+(\frac{b}{\mu}-\frac{z^*}{1-\eta})\beta-(\frac{a}{\mu}-\frac{z}{1-\eta})\beta^*+\frac{\tau}{2}(\beta^2+\beta^{*2})\Big)\Big]_{a=0,b=0}\\
&= \frac{A_2^m e^{\frac{|z|^2}{1-\eta}}}{\mu\sqrt{\eta^2-\tau^2(1-\eta)^2}}W_0(z,z^*,\eta)\partial_a^m\partial_b^m\Big[e^{A_2a^2+B_2a+B_2^*-D_2ab+A_2b^2}\Big]_{a=0,b=0}\\
&= \frac{A_2^m e^{\frac{|z|^2}{1-\eta}}}{\mu\sqrt{\eta^2-\tau^2(1-\eta)^2}}W_0(z,z^*,\eta)\sum_{k=0}^{m}(-1)^{m-k}\frac{m!}{k!(m-k)!}\Big(\frac{D_2}{A_2}\Big)^k L_{m-k}\Big(\frac{|B_2|^2}{4A_2}\Big).
\end{aligned} \tag{26}$$

where,

$$W_0(z,z^*,\eta) = exp\Big(-\frac{\frac{\eta}{1-\eta}|z|^2-\frac{\tau}{2}(z^2+z^{*2})}{\eta^2-\tau^2(1-\eta)^2}\Big)$$
$$A_2 = \frac{A_1}{\mu^2}-\frac{\tau}{2},\ B_2 = \frac{B_1}{\mu},\ D_2 = \frac{D_1}{\mu^2} \tag{27}$$

Using the technique discussed in appendix A, we calculate the Wigner function for PASVS and SNS.

Appendix B: $W(z,z^*)$ for PASVS and SNS

Wigner distribution for any density operator is given as,

$$W(z,z^*) = 2e^{2|z|^2}\int\frac{d^2\beta}{\pi}\langle-\beta|\psi_{\rm SNS}\rangle\langle\psi_{\rm SNS}|\beta\rangle e^{2(z\beta^*-z^*\beta)}. \tag{28}$$

Thus, the Wigner distribution for PASVS and SNS are given as,

$$W_{\rm PASVS}(\alpha,\alpha^*) = 2e^{2|\alpha|^2}\int\frac{d^2\beta}{\pi}\langle-\beta|\psi_{\rm PASVS}\rangle\langle\psi_{\rm PASVS}|\beta\rangle e^{2(\alpha\beta^*-\alpha^*\beta)}$$

$$\begin{aligned}
&= \frac{2e^{2|\alpha|^2}}{N_m\mu}\int\frac{d^2\beta}{\pi}e^{-|\beta|^2+2(\alpha\beta^*-\alpha^*\beta)}\partial_p^m\Big[\int\frac{d^2\gamma}{\pi}e^{-|\gamma|^2-\beta^*\gamma+p\gamma^*+\frac{\tau}{2}\gamma^{*2}}\Big]_{p=0}\partial_q^m\Big[\int\frac{d^2\eta}{\pi}e^{-|\eta|^2+q\eta+\beta\eta^*+\frac{\tau}{2}\eta}\Big]_{q=0}\\
&= \frac{2e^{2|\alpha|^2}}{N_m\mu}\partial_p^m\partial_q^m\Big[\frac{1}{\sqrt{1-\tau^2}}e^{\frac{1}{1-\tau^2}\Big(-(p-2\alpha)(q-2\alpha^*)+\frac{\tau}{2}\overline{(p-2\alpha)^2+(q-2\alpha^*)^2}\Big)}\Big]_{p=0,q=0}
\end{aligned}$$

$$= \frac{2e^{2[(\mu^2+\nu^2)|\alpha|^2-\mu\nu(\alpha^2+\alpha^{*2})]}}{N_m}\partial_p^m\partial_q^m\Big[e^{\frac{\mu\nu}{2}(p^2+q^2)-\mu^2pq+2\mu\overline{q(\mu\alpha-\nu\alpha^*)+p(\mu\alpha^*-\nu\alpha)}}\Big]_{p=0,q=0}$$
$$= \frac{2(-1)^m m! e^{-2|\beta|^2}\mu^m\nu^m}{2^m N_m}\Sigma_{k=0}^m\frac{m!(\frac{\tau}{2})^{-k}}{k!(m-k)!}L_{m-k}\Big(\frac{2|\beta|^2}{\tau}\Big). \quad (29)$$

$$W_{\rm SNS}(\alpha,\alpha^*) = 2e^{2|\alpha|^2}\int\frac{d^2\beta}{\pi}\langle-\beta|\psi_{\rm SNS}\rangle\langle\psi_{\rm SNS}|\beta\rangle e^{2(\alpha\beta^*-\alpha^*\beta)}$$
$$= \frac{2e^{2|\alpha|^2}}{m!\mu}\partial_p^m\partial_q^m\Big[e^{-\frac{\tau}{2}(p^2+q^2)}\int\frac{d^2\beta}{\pi}e^{-|\beta|^2+(\frac{q}{\mu}-2\alpha^*)\beta-(\frac{p}{\mu}-2\alpha)\beta^*+\frac{\tau}{2}(\beta^2+\beta^{*2})}\Big]_{p=0,q=0}$$
$$= \frac{2e^{2[(\mu^2+\nu^2)|\alpha|^2-\mu\nu(\alpha^2+\alpha^{*2})]}}{m!}\partial_p^m\partial_q^m\Big[e^{-pq+2q(\mu\alpha-\nu\alpha^*)+2p(\mu\alpha^*-\nu\alpha)}\Big]_{p=0,q=0}$$
$$= 2(-1)^m e^{-2|\beta|^2}L_m(4|\beta|^2). \quad (30)$$

where $\mu = cosh(r), \nu = sinh(r), \beta = \mu\alpha - \nu\alpha^*$. Evidently for $\eta = \frac{1}{2}$, Eq. (19) and (22) coincide with Eq. (25a) and (25b) respectively, since for $\eta = \frac{1}{2}$, $R(z,\eta)$, coincides with the respective Wigner function, $W(z,z^*)$.

* Electronic address: soumyakanti@bose.res.in
† Electronic address: sanjay@bose.res.in

[1] M. Nielsen and I. Chuang, *Quantum Computation and Quantum Information*, (10^{th} Anniversary Edition, Cambridge University Press, UK, 2010)
[2] W. P. Schleich, *Quantum Optics in Phase Space*, (1^{st} Edition, Wiley-VCH, Berlin, 2001)
[3] M. S. Kim, W. Son, V. Buzek and P. L. Knight, Phys. Rev. A **65**, 032323 (2002)
[4] Wang Xiang-bin, Phys. Rev. A **66**, 024303 (2002); J. S. Ivan, *et al.*, Phys. Rev. A **83**, 032118 (2011)
[5] R. J. Galuber, Phys. Rev. **131**, 2766 (1963)
[6] L. Mandel, Phys. Scr. **12**, 34 (1986)
[7] G. S. Agarwal and K. Tara, Phys. Rev. A **43**, 492 (1991); G. S. Agarwal and K. Tara, Phys. Rev. A **46**, 485 (1992); A. R. Usha Devi, R. Prabhu and M. S. Uma, Eur. Phys. J. D **40**, 133 (2006)
[8] H. P. Yuen, Phys. Rev. A **13**, 2226 (1976)
[9] Y. Yamamoto, N. Imoto and S. Machida, Phys. Rev. A **33**, 3243 (1986)
[10] G. S. Agarwal and J. Banerji, J. Phys. A:Math. Gen. **39**, 11503 (2005); Xun-Li Feng, Ru-Xin Li and Zhi-Zhan Xu, Phys. Rev. A **71**, 032335 (2005); R. Tahira, M. Ikram, H. Nha and M. S. Zubairy, Phys. Rev. A **79**, 023816 (2009)
[11] J. K. Asboth, J. Calsamiglia and H. Ritsch, Phys. Rev. Lett. **94**, 173602 (2005)
[12] M. S. Kim, F. A. M. de Oliveira and P. L. Knight, Phys. Rev. A **40**, 2494 (1989)
[13] Z Zhang and H Fan, Phys. Lett. A **165**, 14 (1992)
[14] P. Král, J. Mod. Opt. **37**, 889 (1990)
[15] Zong-Zheng Xin *et al.*, J. Phys. B: At. Mol. Opt. Phys. **29**, 4493 (1996)
[16] V. I. Man'ko and A. Wünsche, Quantum Semiclass. Opt. **9**, 381 (1997)
[17] L.Y. Hu and H.Y. Fan, J. Mod. Opt, **57**, 1344 (2010)
[18] Su-Youg Lee, Se-Wan Ji, Ho-Joon Kim and H. Nha, Phys. Rev. A **84**, 012302 (2011); C. Navarrete-Benlloch, R. Garcia-Patron, J. H. Shapiro and N. J. Cerf, Phys. Rev. A **86**, 012328 (2012)
[19] J. Adesso and F. Illuminati, J. Phys. A:Math. Theor. **40**, 7821 (2007); F. Dell'Anno, S. De Siena, L. Albano and F. Illuminati, Phys. Rev. A **76**, 022301 (2007); Yang Yang and Fu-Li Li, Phys. Rev. A **80**, 022315 (2009); F. Dell'Anno, S. De Siena and F. Illuminati, Phys. Rev. A **81**, 012333 (2010)
[20] S. Rahimi-Keshari, T. Kiesel, W. Vogel, S. Grandi, A. Zavatta, and M. Bellini, Phys. Rev. Lett. **110**, 160401 (2013)
[21] M. S. Kim, F. A. M. de Oliveira and P. L. Knight, Opt. Commun. **72**, 99 (1989)
[22] C. T. Lee, Phys. Rev. A(R) 44, 2775 (1991)
[23] N. Lutkenhaus and S. M. Barnett, Phys. Rev. A **51**, 3340 (1995)
[24] A. Kenfack and K. Zyczkowski, J. Opt. B:Quantum Semiclass. Opt. **6**, 396 (2004)
[25] V. V. Dodonov, O. V. Man'ko, V. I. Man'ko and A. Wünsche, J.Mod.Opt. **47**, 633 (2000)
[26] M. Hillery,Phys. Lett. A **111**, 409 (1985)
[27] M. Kitagawa and Y. Yamamoto, Phys. Rev. A. **34**, 3974 (1986)
[28] C. M. Caves Phys. Rev. D. **23**, 1693 (1981)